International Journal of Engineering & Applied Sciences (IJEAS)
Vol. 12, Issue 1 (2020) 43-56
http://dx.doi.org/10.24107/ijeas.727320
Int J Eng Appl Sci 12(1) (2020) 43-56

Buckling Analysis of Functionally Graded Plates Using Finite Element Analysis

Nihat CAN [a], Naci KURGAN [b], Ahmed HASSAN [c]*

[a,b,c] Department of Mechanical Engineering, Ondokuz Mayıs University,55139, Samsun, Turkey
[*]E-mail address: 13210381@stu.omu.edu.tr [a], naci.kurgan@omu.edu.tr [b], 15210457@stu.omu.edu.tr [c]

ORCID numbers of authors:
0000-0002-5741-0890[a], 0000-0001-7297-7249[b],
0000-0002-4880-0184[c]

Received date: 26.04.2020
Accepted date: 20.05.2020

Abstract

The present study aims to give critical buckling loads of rectangular functionally graded (FG) plates for various types of boundary conditions. The finite element formulation of stability of plates is introduced and the procedure is applied to obtain critical buckling loads of a plate for two types of boundary conditions: (a) CFFC: two parallel edges are clamped and free along the other two; (b) FFFC: the plate is clamped along one edge and free along all the others. Variation of mechanical properties of the FG plate along the length and the variation along the thickness have been both considered. According to the function of elasticity modulus variation, results have been obtained for various power indices of the varying function. Results compare well with those obtained using shell elements in ANSYS.

Keywords: FGM, buckling of plates, finite element method, ANSYS.

1. Introduction

Typical composite structures with a mixture of two or more different material phases can be referred to as functionally graded plates (FG plates) and the performance of the plates is achieved by adjusting the component formula that forms the structure. Such plates completely inherit the properties of their components and have some special properties such as high hardness, high fatigue resistance, wear resistance. For example, ceramic and metal mixed FG plates have thermal properties of ceramics while also having ductility of metals. Therefore, FG plates, aircraft, vehicles, ships and so on. It is widely used in engineering applications including. Generally, FG plates are subjected to different types of mechanical loads depending on the environment in which they operate and are located. In particular, the behavior of the structure under mechanical loads causing static bending and buckling is very important for the design of the structure. Therefore, it is important to examine the static bending and buckling behavior of FG plates.

Levy [1] proposed a method to demonstrate the buckling behavior of rectangular plates subjected to lateral pressure and edge compression. Javaheri and Eslami [2] investigated the buckling analysis of functionally graded plates under in-plane compression loads based on classical plate theory. Chen and Liew [3] presented buckling analysis using a net method to determine the critical buckling loads of functionally graded rectangular plates exposed to nonlinear loads at plane edge loads. Vel and Batrab [4] developed a three-dimensional precise solution for simply supported free and forced vibrations of functionally graded rectangular plates. Chi and Yen [5], a functionally classified rectangular material plate with simple constrained conditions subjected to transverse loading. Shariah and Eslami [6] obtained a closed-form solution to the buckling of the FG plate, based on the theory that the plate was loaded with mechanical, thermal loads and bending loads for third order shear deformation. Modeling and analysis of functionally classified material plates was performed by Birman and Larry [7]. An analysis of the classical plate theory and the expansion of the Fourier series was achieved by Using the second-order shear deformation theory, the natural frequency of the functional-grade rectangular plate was estimated by Shahrjerdi et al. [8]. Theoretical analysis of FGM plates based on the physical boundary surface was discussed by Zhangand Zhou [9]. Prakashetal [10] examined the effect of neutral surface position on the nonlinear stability behavior of functionally graded plates using the finite element method. Mohammadi et al. [11] have analytically solved the buckling analysis of simply supported, moderately thick, functionally graded rectangular plates with two opposite sides. Talha and Singh [12] researched the static and free vibration analysis of functionally classified material plates by using finite element model and high-grade shear deformation theory. Pendhari et al. [13] established analytical and mixed semi-analytical static solutions for a simple supported plate that is functionally rated in a rectangular form. Singha et al. [14] utilized the finite element method in the analysis of nonlinear behavior of functionally graded plates under transverse load based on the first order shear deformation theory. Hashemi et al. [15] done the new fully closed form method for free vibration analysis of functionally graded rectangular thick plates, based on Reddy's theory of the third-order shear deformation plate. Bousahla et al. [16] offered a plate theory for the buckling analysis of functionally graded plates subjected to uniform, linear and nonlinear temperature increases throughout the thickness. Demirhan and Taskin [17] submitted Levy's solution, which is based on four variable plate theory, for bending analysis of functionally graded sandwich plates. By Mohseni et al. [18], higher grade shear and normal deformable plate theory was employed for analytical solution of static analysis of functionally graded thick micro-plates. Although there have been many studies on the analysis of isotropic and laminated composite beams (i.e., [19-22]), however, the research effort dedicated to stability analysis of rectangular of FG plates has been very limited.

In this study, stability analysis of rectangular FG plates was carried out using thin plate theory under various boundary conditions. The ceramic-metal (Alumina-Aluminum) composition of the FGM was chosen for numerical results. Using the finite element method, critical buckling loads for two types of boundary conditions were found. These boundary conditions are as follows: 1- The plate is held along the edges to which the load is applied and free at the other edges. 2- The plate was applied to be held along one edge and free along the other three edges. The change in the characteristics of the FG plate was considered in two ways. The model was formed by assuming that the elastic properties of the plate changed along the length of the plate, and that the elastic properties of the plate changed along the thickness of the plate.

2. FGM Structures

In order to analyze FGM structures as shown in Fig. 1, two types of FG variation have been considered. In the first, the elasticity modulus varies according to the function given in the equation $E(x) = (E_1 - E_2)(\frac{x+L}{2L})^n + E_2$. The other variation function is given as $E(x)=E_1e^{-\lambda x}$.

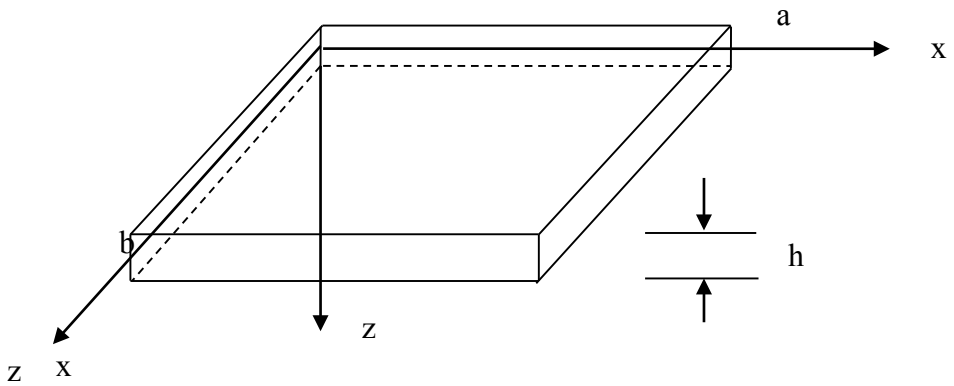

Fig. 1. A Rectangular Plate and Coordinate System

3. Provision of Solution Method

The efficiency and reality of numerical methods is first checked with the analytical results obtained for the square plate homogeneous. In the equations given in $E(x) = (E_1 - E_2)(\frac{x+L}{2L})^n + E_2$ and $E(x)=E_1e^{-\lambda x}$, the cases are related to a functionally graded plate with λ and n factors. If these are chosen to be zero, the plate will be homogenous. Also, when the inclination angle is zero with the λ=0 and n=0 the plate is a square homogenous plate which has the analytical solution given in the literature [23] as $N_x = 10.07\frac{\pi^2 D}{a^2}$; where D is the plate stiffness. To compare the results obtained from FEM and ANSYS a plate with varying thicknesses is used. For a plate with the dimensions a=0.5, h from 0.0005 to 0.005 and E= 380.E+09 GPa. The subscripted terms in Table 1 that is $()_b$ (plate base) and $()_t$ (plate tip) are the material properties of FG rectangular plate. Table 2. shows results from analytical method and finite element method to observe the difference. Note the results are close to each other for the homogenous case.

Table 1. Material properties of the FGM plate.

Properties	Unit	Aluminum; $()_b$	Alumina; $()_t$
E	Pa	70×10^9	380×10^9
υ	---	0,3	0,3

Table 2. Critical buckling loads obtained analytically and by FEM, ANSYS for the homogenous square plate.

h	Critical Buckling Load (N_x) (FEM)	Critical Buckling Load (N_x) (ANALYTICALL)	Critical Buckling Load (N_x) (ANSYS)
0.0005	1734.4789	1729.264	1733.4698
0.001	13875.8309	13834.1123	13874.8219
0.0015	46830.9239	46690.1235	46829.8392
0.002	111006.6472	110672.8982	111005.7647
0.0025	216809.8125	216157.959	216808.7185
0.003	374647.3908	373520.9879	374646.4009
0.0035	594926.2204	593137.5341	594927.4202
0.004	888053.178	885383.1855	888052.872
0.0045	1264434.748	1260633.139	1264433.848
0.005	1734478.5	1729263.672	1734477.6

4. Formulation with FEM and Solution Procedure

Equation of total tensile energy of a rectangular plate:

$$U = \frac{D_{FGM}}{2}\int_{-a}^{a}\int_{-b}^{b}\left\{\left(\frac{\partial_2 w}{\partial x_2}+\frac{\partial^2 w}{\partial y^2}\right)^2 - 2(1-\nu)\left[\left(\frac{\partial^2 w}{\partial x \partial y}\right)^2 - \frac{\partial^2 w}{\partial x^2}\frac{\partial^2 w}{\partial y^2}\right]\right\}dxdy$$
$$-\frac{1}{2}\int_{-a}^{a}\int_{-b}^{b}\left\{N_x\left(\frac{\partial w}{\partial x}\right)^2 + 2N_{xy}\frac{\partial w}{\partial x}\frac{\partial w}{\partial y} + N_y\left(\frac{\partial w}{\partial y}\right)^2\right\}dxdy \quad (1)$$

where the stiffness matrix of FGM plate [D_{FGM}] is

$$[D]_{FGM} = \frac{\mathrm{E}(x)h^3}{12(1-\nu^2)}\begin{bmatrix} 1 & \nu & 0 \\ \nu & 1 & 0 \\ 0 & 0 & \frac{1-\nu}{2} \end{bmatrix} \quad (2)$$

The Elasticity Module, which changes along the X axis, is defined as displacements in a plate: w= off-plane deviation, $\theta_x = \frac{\partial w}{\partial y}$; slope of the plate in the y direction, $\theta_y = \frac{\partial w}{\partial x}$; slope of the plate in the x direction, $\theta_{xy} = \frac{\partial^2 w}{\partial x \partial y}$;

Deformation equivalents are in matrix form:

$$\{\varepsilon\} = \begin{Bmatrix} -\dfrac{\partial^2 w}{\partial x^2} \\ -\dfrac{\partial^2 w}{\partial y^2} \\ -2-\dfrac{\partial^2 w}{\partial x \partial y} \end{Bmatrix} \tag{3}$$

and the stresses are:

$$\{\sigma\} = \begin{Bmatrix} M_x \\ M_y \\ M_{xy} \end{Bmatrix} \tag{4}$$

where

$$M_x = \frac{E(x)h^3}{12(1-\nu^2)}\left(-\frac{\partial^2 w}{\partial x^2} - \nu\frac{\partial^2 w}{\partial y^2}\right) \qquad M_y = \frac{E(x)h^3}{12(1-\nu^2)}\left(-\frac{\partial^2 w}{\partial y^2} - \nu\frac{\partial^2 w}{\partial x^2}\right)$$

$$M_{xy} = (1-\nu)\frac{E(x)h^3}{12(1-\nu^2)}\left(-\frac{\partial^2 w}{\partial x \partial y}\right) \tag{5}$$

since modulus of elasticity varies along the x-axis.
Therefore, stresses are in matrix form:

$$\{\sigma\} = \begin{Bmatrix} M_x \\ M_y \\ M_{xy} \end{Bmatrix} = [\mathrm{D}]_{FGM}\ \{\varepsilon\} = [\mathrm{D}]_{\mathrm{FGM}} \begin{Bmatrix} -\dfrac{\partial^2 w}{\partial x^2} \\ -\dfrac{\partial^2 w}{\partial y^2} \\ -2-\dfrac{\partial^2 w}{\partial x \partial y} \end{Bmatrix} \tag{6}$$

On the other hand, the total tensile energy equation of a rectangular plate at loads thought to be applied only to N_x's:

$$U = \iint_R \left(M_x\left(\frac{\partial^2 w}{\partial x^2}\right) + 2M_{xy}\left(\frac{\partial^2 w}{\partial x \partial y}\right) + M_y\left(\frac{\partial^2 w}{\partial y^2}\right)\right)dxdy + \iint_R \left(N_x \frac{\partial^2 w}{\partial x^2}\right)dxdy \tag{7}$$

Taking the first variation of the energy equation above, writing equal to zero and in matrix form:

$$U = \iint_R \left(\begin{bmatrix} M_x & M_y & M_{xy} \end{bmatrix} \delta \begin{Bmatrix} -\dfrac{\partial^2 w}{\partial x^2} \\ -\dfrac{\partial^2 w}{\partial y^2} \\ -2-\dfrac{\partial^2 w}{\partial x \partial y} \end{Bmatrix} \right) dxdy + \iint_R N_x \frac{\partial w}{\partial x} \delta \left(\frac{\partial w}{\partial x} \right) dxdy = 0 \tag{8}$$

by using Equations (5) and (6) and (8) this statement can be written as:

$$U = \iint_R \{\delta\varepsilon\}^T \frac{\mathrm{E}_1 e^{-\lambda x} h^3}{12(1-\nu^2)} \begin{bmatrix} 1 & \nu & 0 \\ \nu & 1 & 0 \\ 0 & 0 & \dfrac{1-\nu}{2} \end{bmatrix} \{\varepsilon\} dxdy + \iint_R N_x \frac{\partial w}{\partial x} \delta \left(\frac{\partial w}{\partial x} \right) dxdy = 0 \tag{9}$$

Hereinafter, the standard Finite Element procedure using Hermitian polynomials will be used. The following definitions are used to represent the Eq. (9) in nodal displacements, including the shape functions $\tilde{N}$'s generated from the Hermitian polynomials:

$$\{w\} = \left[\tilde{N}\right]\{a\} = \{a\}^T \left[\tilde{N}\right]^T \tag{10}$$

and

$$\delta w = \{\delta a\}^T \left[\tilde{N}\right]^T \tag{11}$$

where T means the transpose of a matrix and $\{a\}$ is the nodal displacement vector.
So, the node displacement vector for an element would be:

$$\{a\}^e = \begin{Bmatrix} a_i \\ a_j \\ a_k \\ a_l \end{Bmatrix} = \begin{Bmatrix} w \\ \theta_x \\ \theta_y \\ \theta_{xy} \\ . \\ . \\ . \end{Bmatrix} \tag{12}$$

Crucial ε as in the form $\{\varepsilon\} = [L]\{w\}$ and $[B] = [L]\left[\tilde{N}\right]$. Hence $\{\varepsilon\} = [B]\{a\}$

Substituting the above equation in Eq. (12) gives

$$\{\delta a\}^T \left(\iint_R [B]^T D_{FGM} \begin{bmatrix} 1 & \nu & 0 \\ \nu & 1 & 0 \\ 0 & 0 & \dfrac{1-\nu}{2} \end{bmatrix} [B] dxdy \right) \{a\} - \{\delta a\}^T \left[\iint_R \left(\left[\tilde{N}_{,x}\right]^T \left[\tilde{N}\right] dxdy \right) \{a\} \right] = 0 \tag{13}$$

Thus, the finite element equation will be in the compact form

$$\left[K_F\right]_{fgm}\{a\} - N_x\left[K_{Gx}\right]\{a\} \tag{14}$$

embodying an eigenvalue problem. $[K_F]$ and $[K_{Gx}]$ are Bending and geometric hardness matrices of FGM plate. Here, the modulus of elasticity of the plate and hence the stiffness matrix [D] must be calculated at the nodes due to its dependence on the x values. Thus, when finite elements are mounted on spherical matrices, the effect of the diversity of the modulus of flexibility is achieved by inserting it into it. But, changing the value λ to zero would be a homogeneous plate where the plate is clearly equal to E_0 along the elastic modulus.
For each element $[K_F]$ and $[K_{Gx}]$ as transmuted into a unit reference element there is

$$\left[K_F\right]^e = \int_{\eta=0}^{1}\int_{\xi=0}^{1}\left[B\right]^T D_{FGM}\begin{bmatrix} 1 & \nu & 0 \\ \nu & 1 & 0 \\ 0 & 0 & \dfrac{1-\nu}{2} \end{bmatrix}\left[B\right]\det\left(J\right)d\xi d\eta\,. \tag{15}$$

[B] matrix is described in shape functions and transformation matrices as:

$$\left[B\right] = \begin{Bmatrix} \left\langle \dfrac{\partial^2 N_0}{\partial x^2} \right\rangle \\ \left\langle \dfrac{\partial^2 N_0}{\partial y^2} \right\rangle \\ \left\langle \dfrac{\partial^2 N_0}{\partial x \partial y} \right\rangle \end{Bmatrix} = \left[T_1\right]\begin{Bmatrix} \left\langle \dfrac{\partial N_0}{\partial \xi} \right\rangle \\ \left\langle \dfrac{\partial N_0}{\partial \eta} \right\rangle \end{Bmatrix} + \left[T_2\right]\begin{Bmatrix} \left\langle \dfrac{\partial^2 N_0}{\partial \xi^2} \right\rangle \\ \left\langle \dfrac{\partial^2 N_0}{\partial \eta^2} \right\rangle \\ \left\langle \dfrac{\partial^2 N_0}{\partial \xi \partial \eta} \right\rangle \end{Bmatrix} \tag{16}$$

where

$$\left[T_2\right] = \begin{bmatrix} j_{11}^2 & j_{12}^2 & 2j_{11}j_{12} \\ j_{21}^2 & j_{22}^2 & 2j_{21}j_{22} \\ j_{11}j_{21} & j_{12}j_{22} & j_{11}j_{22} + j_{12}j_{21} \end{bmatrix} \tag{17}$$

and

$$\left[T_1\right] = -\left[T_2\right]\begin{bmatrix} \dfrac{\partial}{\partial \xi}J_{11} & \dfrac{\partial}{\partial \xi}J_{12} \\ \dfrac{1}{2}\left(\dfrac{\partial}{\partial \eta}J_{11} + \dfrac{\partial}{\partial \xi}J_{21}\right) & \dfrac{1}{2}\left(\dfrac{\partial}{\partial \eta}J_{12} + \dfrac{\partial}{\partial \xi}J_{22}\right) \end{bmatrix}\left[j\right] \tag{18}$$

In the above equations the J_{ij} and j_{ij} are the elements Jacobian and inverse Jacobian matrices of the transformation respectively. For two dimensional transformation the elements of Jacobian matrix are $J_{11} = \partial x / \partial \xi$, $J_{12} = \partial y / \partial \xi$, $J_{21} = \partial x / \partial \eta$, $J_{22} = \partial y / \partial \eta$.
As the flexural stiffness matrix $[K_F]$ carries the effect of the elasticity modulus change the geometric rigidity matrix $[K_{Gx}]$ carries the effect of the plate's and considering the equilibrium of the forces will be in the form:

$$[K_{Gx}]^e = \int_{\eta=0}^{1}\int_{\xi=0}^{1} \frac{b_1}{b_1 + 2x\tan\theta}\left(j_{11}N_\xi + j_{12}N_\eta\right)\left\langle j_{11}N_\xi + j_{12}N_\eta\right\rangle d\xi d\eta \tag{19}$$

The coordinate x in the real plane is also transformed into the reference plane in both $[K_F]$ and $[K_{Gx}]$ matrices by $x = (\xi-1)(\eta-1)x_1 - \xi(\eta-1)x_2 + \xi\eta x_3 - \eta(\xi-1)x_4$ attained from the transformation polynomials. Here x_1,.., x_4 are the x coordinates of a real element. In Equation (19) simple taking the θ value as zero reach the geometric matrix of a rectangular plate.
Varying elasticity modulus along z-axis to obtain the effect of the change of elasticity modulus along the thickness the same procedure is applied but this time the [D] matrix of the FGM plate includes the integral of the elasticity modulus along the z-axis. Thus, Eq. (2) will be in the form if an E(z) function as in the Equation $E = (E_t - E_b)\left(\frac{2z+h}{2h}\right)^n + E_b$:

$$[D]_{fgm} = \frac{1}{(1-\nu^2)}\begin{bmatrix} 1 & \nu & 0 \\ \nu & 1 & 0 \\ 0 & 0 & \frac{1-\nu}{2} \end{bmatrix} \int_{-h/2}^{h/2} \left\{(E_1 - E_2)(\frac{2z+h}{2h})^n + E_2\right\} z^2 dz \tag{20}$$

Although the integral along the z-axis can be calculated analytically as

$$\int_{-h/2}^{h/2} \left\{(E_1 - E_2)(\frac{2z+h}{2h})^n + E_2\right\} z^2 dz \tag{21}$$

$$= \frac{(E_1 - E_2)h^3}{1-\nu^2}\frac{n^2+n+2}{4(n+1)(n+2)(n+3)} + \frac{E_2 h^3}{12(1-\nu^2)}$$

it is convenient to calculate its value by any of the numerical integral methods such as Gaussian Quadrature method to provide its applicability to a numerical computation [24]. This time in the Equation (20) E_1 and E_2 denotes the upper and lower surfaces' elasticity modulus of the plate respectively. The effect of the elasticity modulus change in the z-direction is inserted by the $[D]_{fgm}$ matrix. Obviously, choosing n=0 the results pertaining to a homogenous case can be reached for the plate which has the elasticity modulus E_1.
Thus the flexural stiffness matrix will be as

$$[K_F]^e = \int_{\eta=0}^{1}\int_{\xi=0}^{1} [B]^T [D]_{fgm} [B] \det(J) d\xi d\eta \tag{22}$$

For the geometric stiffness matrix $[K_{Gx}]$ of the trapezoidal plate Equation (19) is still valid.

5. Results and Discussions

Figures (2,7) show comparison of FEM and ANSYS evolution of critical buckling loads N_x of FGM plate power law index n with aspect ratio a/b=0.25;0.5;0.75;1.0 at CFFC and FFFC boundary conditions for the elasticity modulus varies according to the function $E(x) = (E_1 - E_2)(\frac{x+L}{2L})^n + E_2$ and $E(x)=E_1e^{-\lambda x}$. Results pertaining to a rectangular FGM plate have been investigated first for various variation of elasticity modulus both along the thickness and along the x-axis. Ceramic-metal material composition of FGM plate has been selected due to fact that this configuration finds plentiful application in the industry. When ceramic side is selected to be alumina the elasticity modulus E=380x10^9 GPa and Poisson's ratio υ=0.3 In addition to this the metal side has properties E=70x10^9 GPa and υ=0.3 when the metal is aluminum. Various ceramic-metal configurations can be selected for various applications. In order to find the effect of these indices on the stability of the FGM plate, buckling of loads against power indices λ and n is given. According to the material and geometric properties used in numerical method model, commercial (ANSYS) finite element code is produced by comparing [25]. Shell models are applied to illustrate how plane mesh size affects the accuracy of buckling analysis for plates of various length ratios and thicknesses in ANSYS. In the finite element model, the Shell281 element is used with various values of plane mesh size, expressed as element per plate edge, and in various thickness values, expressed as the half-thickness ratio up to thin to medium FGM plates. The Shell281 model uses the observation size of 80 and 100 elements per side for each side thickness ratio. The variations of critical buckling loads in FGM*)* plate for different boundary conditions are shows in Fig.2-7. The effect of power law index n and λ on the critical buckling loads can be seen for different boundary conditions. Figs.2-7 shows the critical buckling loads verses power law index value at different boundary conditions. As expected, the increasing index value leads to reduce the critical buckling loads. Increasing index value reduces the ceramic constituents, it produces the effective material properties changes which affect the critical buckling loads.

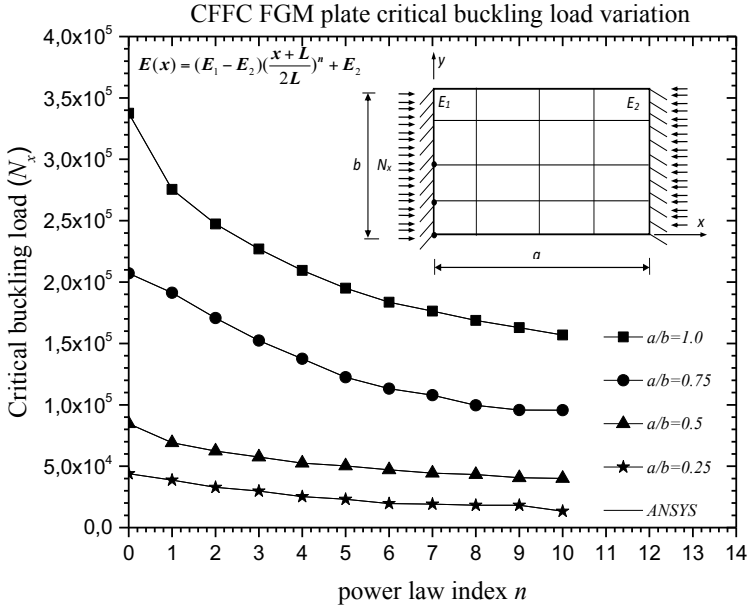

Fig. 2. Critical buckling load of FGM plate verses power law index n with aspect ratio a/b=0.25;0.5;0.75;1.0 at CFFC boundary conditions for the elasticity modulus varies according to the function $E(x) = (E_1 - E_2)(\frac{x+L}{2L})^n + E_2$

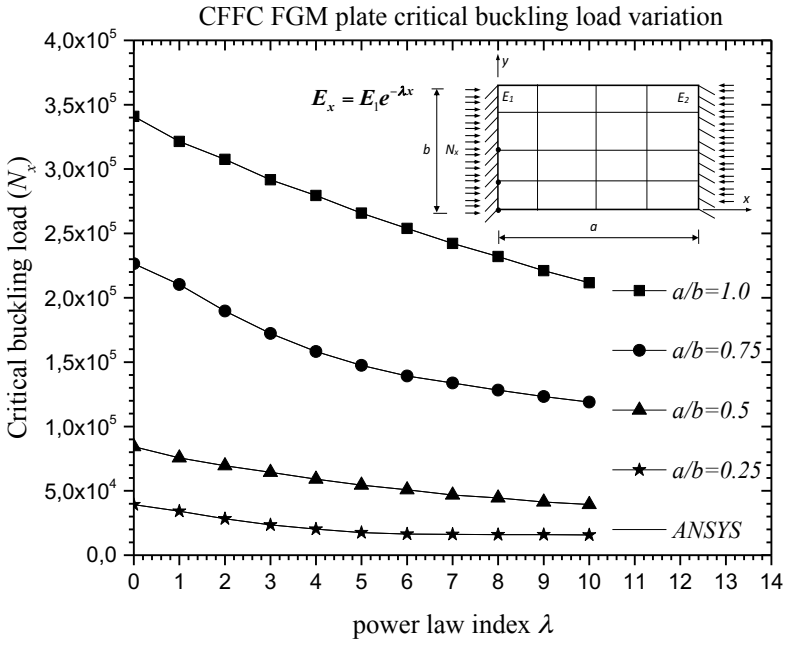

Fig. 3. Critical buckling load of FGM plate verses power law index λ with aspect ratio a/b=0.25;0.5;0.75;1.0 at CFFC boundary conditions for the elasticity modulus varies according to the function $E(x)=E_1e^{-\lambda x}$

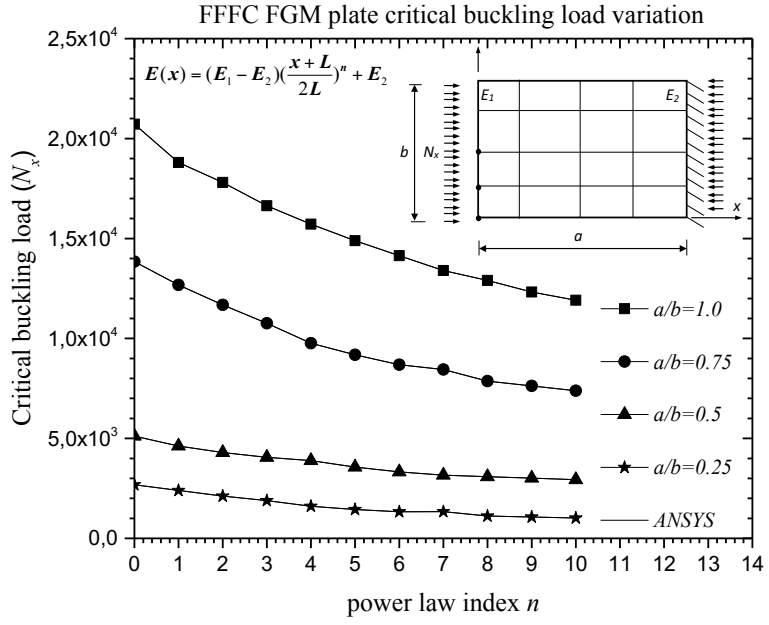

Fig. 4. Critical buckling load of FGM plate verses power law index n with aspect ratio a/b=0.25;0.5;0.75;1.0 at FFFC boundary conditions for the elasticity modulus varies according to the function $E(x) = (E_1 - E_2)(\frac{x+L}{2L})^n + E_2$

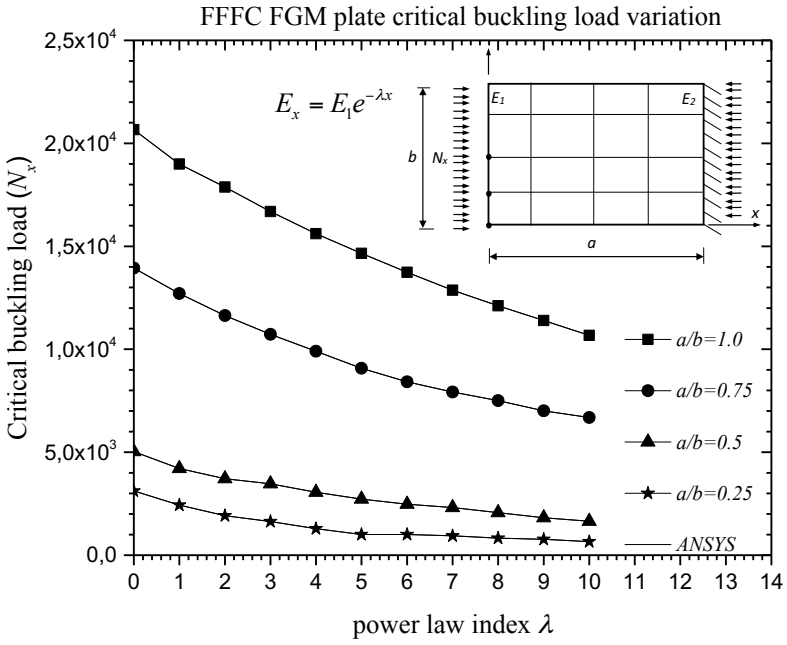

Fig. 5. Critical buckling load of FGM plate verses power law index λ with aspect ratio a/b=0.25;0.5;0.75;1.0 at FFFC boundary conditions for the elasticity modulus varies according to the function $E(x)=E_1 e^{-\lambda x}$

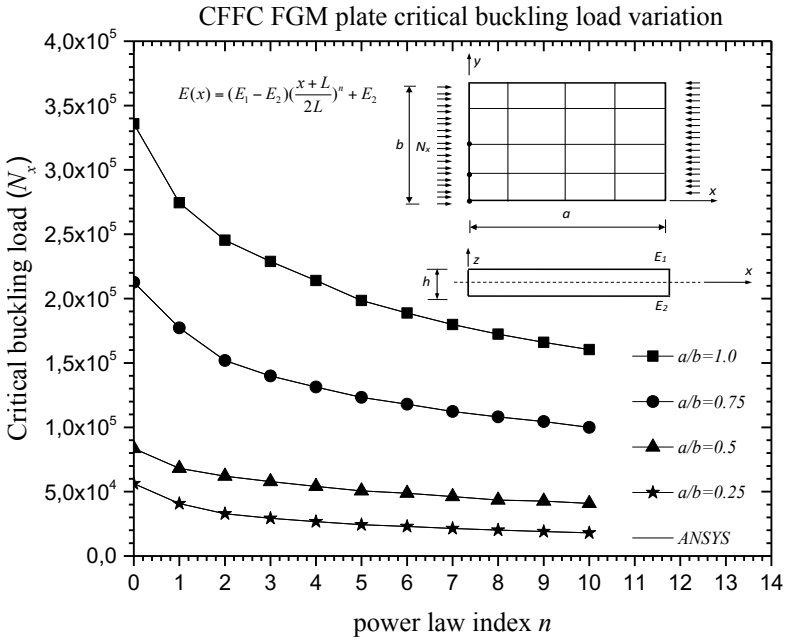

Fig. 6. Critical buckling load of FGM plate verses power law index n with aspect ratio a/b=0.25;0.5;0.75;1.0 at CFFC boundary conditions for the elasticity modulus varies according to the function $E(x) = (E_1 - E_2)(\frac{x+L}{2L})^n + E_2$

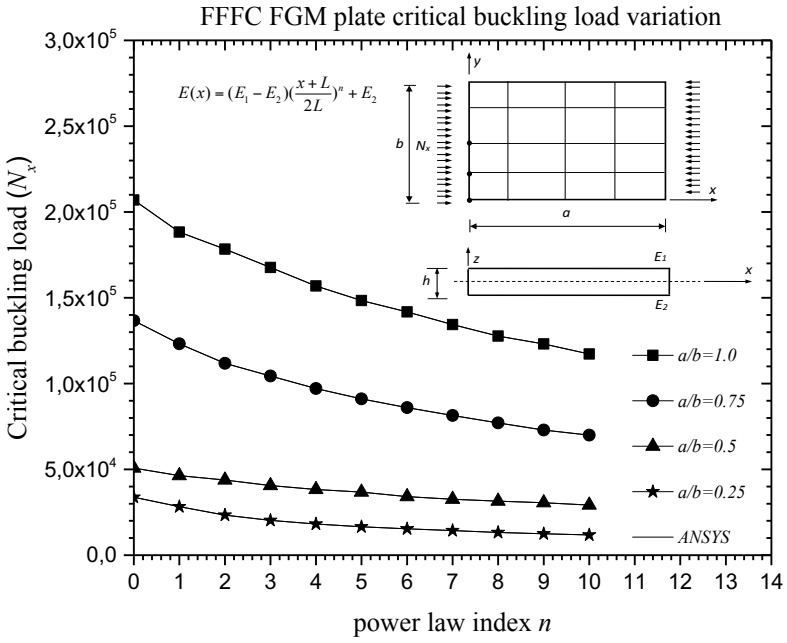

Fig. 7. Critical buckling load of FGM plate verses power law index n with aspect ratio a/b=0.25;0.5;0.75;1.0 at FFFC boundary conditions for the elasticity modulus varies according to the function $E(x) = (E_1 - E_2)(\frac{x+L}{2L})^n + E_2$

6. Conclusion

The stability behavior of rectangular FGM plates under various boundary conditions is investigated using the finite element method. The ceramic-metal (Alumina-Aluminum) composition of FGM has been chosen to obtain numerical results. Two types of boundary conditions have been studied CFFC configuration and FFFC configuration. In order to justify the proposed model, a homogeneous rectangular plate condition is considered. The results obtained for the CFFC configuration were observed to have lower critical buckling loads than those obtained for the FFFC configuration. The latter is less stable. This applies to both homogeneous and FGM plates. Increasing the power law indices (λ and n) makes the plate less stable. At large values of these indices, the plate achieves an unstable behavior as if there were no restrictions along the plates and thus buckles easily. This negative impact of the power index should be considered during the design of the structures. The effect of the metal-ceramic composition (the properties of the components of the FGM plate), the power law indices determining the amount of the composition, the dimensions of the plate, the angle of inclination and the boundary conditions affect the stability of the plate. Good configuration of these parameters will ensure that the structure has the optimum critical buckling load value. Although the specified parameters have limitations with respect to each other, optimum configurations can be obtained according to use by observing their effects separately.

References

[1] Levy, S., *Bending of rectangular plates with large deflections*. 1942: US Government Printing Office.

[2] Javaheri, R. and M. Eslami, Buckling of Functionally Graded Plates under In- plane Compressive Loading. *ZAMM- Journal of Applied Mathematics and Mechanics/Zeitschrift für Angewandte Mathematik und Mechanik: Applied Mathematics and Mechanics,* 82, 277-283, 2002

[3] Chen, X. and K. Liew, Buckling of rectangular functionally graded material plates subjected to nonlinearly distributed in-plane edge loads. *Smart Materials and Structures,* 13, 1430, 2004

[4] Vel, S.S. and R. Batra, Three-dimensional exact solution for the vibration of functionally graded rectangular plates. *Journal of Sound and Vibration,* 272, 703-730, 2004

[5] Chi, S.-H. and Y.-L. Chung, Mechanical behavior of functionally graded material plates under transverse load—Part I: Analysis. *International Journal of Solids and Structures,* 43, 3657-3674, 2006

[6] Shariat, B.S. and M. Eslami, Buckling of thick functionally graded plates under mechanical and thermal loads. *Composite Structures,* 78, 433-439, 2007

[7] Birman, V. and L.W. Byrd, Modeling and analysis of functionally graded materials and structures. 2007

[8] Shahrjerdi, A., F. Mustapha, M. Bayat, S. Sapuan, R. Zahari, and M. Shahzamanian. *Natural frequency of FG rectangular plate by shear deformation theory*. in *IOP conference series: materials science and engineering*. 2011. IOP Publishing.

[9] Zhang, D.-G. and Y.-H. Zhou, A theoretical analysis of FGM thin plates based on physical neutral surface. *Computational Materials Science,* 44, 716-720, 2008

[10] Prakash, T., M. Singha, and M. Ganapathi, Influence of neutral surface position on the nonlinear stability behavior of functionally graded plates. *Computational mechanics,* 43, 341-350, 2009

[11] Mohammadi, M., A. Saidi, and E. Jomehzadeh, A novel analytical approach for the buckling analysis of moderately thick functionally graded rectangular plates with two simply-supported opposite edges. *Proceedings of the Institution of Mechanical Engineers, Part C: Journal of Mechanical Engineering Science,* 224, 1831-1841, 2010

[12] Talha, M. and B. Singh, Static response and free vibration analysis of FGM plates using higher order shear deformation theory. *Applied Mathematical Modelling,* 34, 3991-4011, 2010

[13] Pendhari, S.S., T. Kant, Y.M. Desai, and C.V. Subbaiah, Static solutions for functionally graded simply supported plates. *International Journal of Mechanics and Materials in Design,* 8, 51-69, 2012

[14] Singha, M., T. Prakash, and M. Ganapathi, Finite element analysis of functionally graded plates under transverse load. *Finite elements in Analysis and Design,* 47, 453-460, 2011

[15] Hosseini-Hashemi, S., M. Fadaee, and S.R. Atashipour, Study on the free vibration of thick functionally graded rectangular plates according to a new exact closed-form procedure. *Composite Structures,* 93, 722-735, 2011

[16] Bousahla, A.A., S. Benyoucef, A. Tounsi, and S. Mahmoud, On thermal stability of plates with functionally graded coefficient of thermal expansion. *Structural Engineering and Mechanics,* 60, 313-335, 2016

[17] Demirhan, P.A. and V. Taskin, Levy solution for bending analysis of functionally graded sandwich plates based on four variable plate theory. *Composite Structures,* 177, 80-95, 2017

[18] Mohseni, E., A. Saidi, and M. Mohammadi, Bending-stretching analysis of thick functionally graded micro-plates using higher-order shear and normal deformable plate theory. *Mechanics of Advanced Materials and Structures,* 24, 1221-1230, 2017

[19] Akgöz, B. and Ö. Civalek, A size-dependent beam model for stability of axially loaded carbon nanotubes surrounded by Pasternak elastic foundation. *Composite Structures,* 176, 1028-1038, 2017

[20] Civalek, Ö. and O. Kiracioglu, Free vibration analysis of Timoshenko beams by DSC method. *International Journal for Numerical Methods in Biomedical Engineering,* 26, 1890-1898, 2010

[21] Civalek, O. and A. Yavas, Large deflection static analysis of rectangular plates on two parameter elastic foundations. *International journal of science and technology,* 1, 43-50, 2006

[22] Mercan, K., Ç. Demir, and Ö. Civalek, Vibration analysis of FG cylindrical shells with power-law index using discrete singular convolution technique. *Curved and Layered Structures,* 1, 2016

[23] Timoshenko, S. and J. Goodier, *Theory of elasticity 3rd edition*. 1970, New York, McGraw-Hill.

[24] Woo, J. and S. Meguid, Nonlinear analysis of functionally graded plates and shallow shells. *International Journal of Solids and structures,* 38, 7409-7421, 2001

[25] ANSYS, A., V11 Program Documentation. *Ansys Inc., Canonsburg, Pennsylvania*,